Fourier-Transform Raman Spectroscopy Study of the Ovariectomized Rat Model of Osteoporosis

Renato Aparecido de Souza[*,1,2], Diego Pereira Jerônimo[2], Hélio Andrade Gouvêa[2], Murilo Xavier[1,2], Marco Túlio de Souza[3], Humberto Miranda[2], Maira Gaspar Tosato[4], Airton Abrahão Martin[4] and Wellington Ribeiro[2]

[1] *Department of Physical Therapy, Vales do Jequitinhonha e Mucuri Federal University, UFVJM, Rua da Glória, 187, 39100-000, Diamantina, Minas Gerais, Brazil*

[2]*Laboratory of Physiology and Pharmacodynamics, Institute of Research and Development, IP&D, Vale do Paraiba University, UNIVAP, Av. Shishima Hifumi, 2911, 12244-000, São José dos Campos, São Paulo, Brazil*

[3]*Faculty of Medicine, Vale do Sapucaí University, UNIVAS, Av. Pref. Tuany Toledo, 470, 37500-000, Pouso Alegre, Minas Gerais, Brazil*

[4] *Laboratory of Biomedical Vibrational Spectroscopy, Institute of Research and Development, IP&D, Vale do Paraiba University, UNIVAP, Av. Shishima Hifumi, 2911, 12244-000, São José dos Campos, São Paulo, Brazil*

Abstract: The ovariectomized rat model of osteoporosis was studied using FT-Raman spectroscopy on the surface of site-specific bones. Twelve, 3 month old female Wistar rats (230 ± 10 g) were divided into two groups (n = 6 per group), one group was: ovariectomized (OVX) and the other sham-operated (SHAM). The rats were sacrificed to collect samples twelve weeks after the surgical operation. The right femur and tibia as well as the third lumbar vertebra were harvested and subjected to FT-Raman analysis on the following bones sites: femoral neck (FN), femoral mid-shaft (FS), proximal tibial metaphysis (PTM), tibial mid-shaft (TS), and lumbar vertebral body (LVB). Analysis of individual Raman peaks showed site-dependent variations in the bone: the ovariectomy induced lower mineral content (959 cm^{-1}) in trabecular bone sites (FN, PTM and LVB) and higher matrix content (1265 and 1665 cm^{-1}) in cortical bone sites (FS and TS). In addition, a lower mineral to matrix ratio and a higher carbonate/phosphate were observed in the OVX group, which indicated a change in bone chemical content and some degree of remodeling specially in the trabecular bone sites. These data support the hypothesis that FT-Raman spectroscopy can be used to evaluate the bone alterations induced by this experimental model.

Keywords: Vibrational spectroscopy, bone, osteoporosis, ovariectomy, rats.

INTRODUCTION

Osteoporosis is a disabling skeletal disorder characterized by progressive bone mass loss and microarchitecture deterioration of bone tissue which predisposes patients to increased bone fracture risk [1]. Osteoporosis is the most common metabolic bone disorder worldwide and, therefore, is considered as a serious public health concern [2]. More than 200 million people worldwide are currently estimated to suffer from this disease. According to the World Health Organization criteria, 1/3 of the white women older than 65 have osteoporosis and osteoporotic fractures will occur in about 50% of women older than 75 years [3]. In Brazil, one in every five Brazilian women > 50 years of age has already had some kind of osteoporotic fracture [4].

Osteoporosis associated with ovarian hormone deficiency following menopause is by far the most common cause of age-related bone loss [1-3]. Experimental animal models have provided knowledge about aetiology, pathophysiology, and diagnosis, as well as about preventive and therapeutical techniques, regarding postmenopausal osteoporosis (PMO) [5,6]. The ovariectomized (OVX) rat is a well-established model of PMO and the site-specific development of osteoporosis in this model is one of the most reliable biological responses in skeletal research [7]. The OVX rat model is considered an appropriate model for studying female postmenopausal osteoporosis because of the many similarities in their pathophysiological mechanisms. OVX exhibit decreased bone mineral density (BMD), poor trabecular microarchitecture and bone strength, and increased bone turnover rate (resorption exceeding formation) [5-8]. Thus, ovariectomy in rats has been widely used as a model of PMO and has been validated as a clinically relevant model of this condition in humans.

The choice of methods to evaluate bone quality, which is defined as an adequate and functional chemical, structural, and metabolic interaction of its mineral and matrix phases [9], is as important as the choice of the animal model. There has been extensive studies about the bones of OVX rats including the use of peripheral computerized tomography (pQCT), high-resolution microcomputed tomography

*Address correspondence to this author at the Laboratory of Physiology and Pharmacodynamics, Institute of Research and Development, IP&D, Vale do Paraiba University, UNIVAP, Av. Shishima Hifumi, 2911, 12244-000, São José dos Campos, São Paulo, Brazil, Fax: +55-12-3947-1149; E-mail: tatosouza2004@yahoo.com.br

1876-5254/10

(microCT), and Dual X-ray Absorptiometry (DXA) to assess the BMD and bone mineral content (BMC) changes [8,10-12]. Histomorphometry has provided a two-dimensional assessment of bone mass and architecture, and has detected the presence of specific molecules within a cell associated with immunohistochemistry techniques [13,14]. Researchers have used biochemical markers to analyze the mineral homeostasis [15,16] and mechanical testing to evaluate bone strength [17,18]. *In vitro* studies about potential changes in the composition and proliferative capacity of bone cell populations [19] have also been performed.

Although these techniques have been widely used, they are not capable of fully predicting bone strength because they cannot measure the bone microarchitecture and crystal organization or the bone proteins structure. For instance, the DXA, the current gold standard screening model to diagnose osteoporosis in humans, identifies the fracture risk by determination of BMD, which is not related with to the bone matrix phase and is only able to account for 60–70% of bone strength variation [20]. In fact, the bone is a biogenic tissue made up of 60-70% mineral substance, mainly a carbonated form of a finely crystalline calcium phosphate, and 30-40% organic matrix, mainly type I collagen fibrils (85-90%) [21]. Therefore, it is important to delineate how tissue ultrastructure modulates the response of bone to its physical environment through a technique that, in addition to measuring the bone's mineral components, also measures bone collagen quality and quantity.

Recently, vibrational spectroscopy has enjoyed increased success as a technique for studying bone properties [22,23]. Fourier-transform Raman spectroscopy (FT-Raman) is a valuable vibrational spectroscopy technique to investigate functional groups, bonding types and molecular conformations. Vibrational spectra are molecular-structural fingerprints to carefully analyze the positions, intensities, and widths of the bands in the Raman spectra of biological tissues. In this technique, the need for tissue preparation is minimal, the measurement is non-destructive to the tissue, and very small amounts of material can be successfully analyzed [24].

Several works have proposed using Raman spectroscopy for detecting, quantifying, and imaging local variations in the molecular structure of bone [22-29]. The chemical composition of bone tissue can be assessment by the ratios between areas of interest in the spectral Raman bands, for example femoral trabecular bone had a higher carbonate/amide I ratio in fractured rather than in unfractured women, while iliac crest biopsies revealed a higher carbonate/phosphate ratio in cortical bone from woman who had sustained a fracture [25]. Goodyear *et al.* compared cortical and trabecular bone from standard laboratory mice and found that the mineral/matrix ratio and the carbonate/phosphate were significantly greater in cortical bone [26]. An assessment of the relative intensity variation of the phosphate peaks indicated the bone's mineral content and degree of mineralization [22]. Shen *et al.* showed that the predominant Raman peak at 960 cm^{-1} was higher in the control group than in animals with osteoporosis induced by spinal cord injury [27]. Furthermore, at least two more spectroscopic parameters have been evaluated in the Raman spectra of bone: (i) the integrated area of peaks centered at 1070 cm^{-1} band, which indicates the amount of type B carbonate substitution in the mineral crystals [28]; and (ii) the integrated area of peaks centered at 1005 cm^{-1} band, which indicates the phosphoprotein that occur in low mineralization regions [29].

No specific information could be found in the literature, which used female rats as a model of osteoporosis, about the ovariectomy effects, on bone microarchitecture and chemical composition at the molecular level that analyzed various bone sites and different bone types. Therefore, this study aimed to investigate the ovariectomized rat model of PMO using FT-Raman spectroscopy to characterize the mineral and matrix phases on the following bones site: femoral neck (FN), femoral mid-shaft (FS), proximal tibial metaphysis (PTM), tibial mid-shaft (TS), and lumbar vertebral body (LVB). Such data are fundamental to clearly understand the effects of this model on local bone composition variations at the molecular level by providing valuable insight about the chemical makeup of altered bone and contributing to PMO healing search.

MATERIALS AND METHODOLOGY

Animal Model and Induction of Osteoporosis

This study was conducted according to the Ethical Principles on Animal Experimentation adopted by the Brazilian College of Animal Experimentation (COBEA) and was approved by Committee for Ethics in Animal Research of the Universidade do Vale do Paraíba (Protocol n^{o} A37/ CEP/2008). Twelve female Wistar rats (*Rattus norvegicus*), weighing 230 ± 10 g were obtained from the Bem-Te-Vi Farm (Paulínia, SP, Brazil) at ~76 days of age and allowed to acclimate for 2 weeks in the bioterium of the Physiology and Pharmacodynamics Laboratory (IP&D, UNIVAP, São José dos Campos. SP, Brazil).

At 3 months of age, the animals (skeletally mature) were weight-matched before surgery. Half were submitted to bilateral ovariectomy (OVX group; n=6) and the other half, to a sham surgery to simulate surgical stress (SHAM group; n=6). The ovariectomy was made under general anesthesia (2% Xylazine hydrochloride, 10 mg/kg, Rompun Bayer, São Paulo, SP, Brazil; and Ketamine, 80 mg/kg, Francotar, Virbac, Roseira, SP, Brazil) by two dorso-lateral incisions below the last ribs and approximately 1 cm long above the ovaries. With the use of a sharp dissecting scissors, the skin was cut together with the dorsal muscles and the peritoneal cavity was thus accessed. After peritoneal cavity was accessed, the ovary was found, surrounded by a variable amount of fat. In the OVX group, hemostasis was performed by ligation of the upper part of the Fallopian tube with #4.0 catgut suture and the ovaries were excised together with surrounding fat, the oviduct, and a small portion of the uterus. The muscle incision required no suturing. Skin wounds were closed bilaterally with #4.0 silk suture. In the SHAM group, the ovaries were exposed but not removed. After surgery or sham-operation, all animals received meloxicam (1 mg/kg) for pain management during first experimental week and were housed in pairs in standard cages within a room maintained at 22 ± 3°C on 12-h light/12-h dark cycles and left untreated for 12 weeks to induce osteoporosis [8]. Throughout the 14 weeks of the

experiment, the OVX and SHAM animals had free access to water and food (standard laboratory diet, Labcil®, Nutri Forte, Uberaba, MG, Brazil).

Specimen Preparation

After 12 weeks of bilateral ovariectomy or sham-operation, all rats were humanely sacrificed with an overdose of general anesthetics and bones (the right femur and tibia, as well as the third lumbar vertebra) were harvested, cleaned of soft tissue, and frozen at −89°C until Raman analysis.

Prior to FT-Raman study, the samples were warmed gradually to room temperature and the surface of site bones were adequately positioned in the spectrometer without any manipulation treatment (chemical fixation or cuts). In order to explain the site-specific development of osteoporosis the following site bones were assessed: femoral neck (FN), femoral mid-shaft (FS), proximal tibial metaphysis (PTM), tibial mid-shaft (TS), and vertebral body of the third lumbar vertebra (LVB).

FT-Raman Spectroscopy Analysis

The FT-Raman spectrometer (RFS 100/S®-Bruker, Inc., Karlsruhe, Germany) with a germanium detector cooled by liquid N_2 was used to collect the data. The samples were excited by an air-cooled Nd:YAG laser (λ=1064.1 nm). The power of the Nd:YAG laser incident on the sample was 183 mW. The spectral resolutions was set to 4 cm^{-1} and for each site bone three spectra (10 μm distance between each point) were collected with 200 scans, totaling 180 spectra. Data collection and data transfer were automated using the Bruker OPUS™ software. Before the spectra treatment, the averages of the three spectra per bone site were performed, resulting into 90 spectra. To remove the fluorescence background from the original spectrum, a fourth order polynomial fitting was found to give better results by faciliting the visualization of the peaks in the interested region (800-1800 cm^{-1}). This procedure was performed by Matlab 6.0® software (Newark, New Jersey, USA).

The spectra treatment were then calculated by the Microcal Origin5.0® software (Microcal Software, Inc., Northampton, MA, USA) and the changes of the mineral content and collagen matrix were analyzed by the following Raman spectroscopic parameters: integrated intensities from Raman peaks 422-454 cm^{-1} (Phosphate: PO_4^{3-} v_2), 578-617 cm^{-1} (Phosphate: PO_4^{3-} v_4), 957-962 cm^{-1} (Phosphate: PO_4^{3-} v_1), 1003-1005 cm^{-1} (v_1 mode of the organic phosphate), 1006-1055 cm^{-1} (Phosphate: PO_4^{3-} v_3), 1065-1071 cm^{-1} (Carbonate: CO_3^{2-} v_1), 1243-1269 cm^{-1} (Amide III), 1447-1452 cm^{-1} (CH_2 wag), and 1595-1720 cm^{-1} (Amide I) [22]. The ratios of these bands areas measured phosphate v_1/Amide I, carbonate v_1/phosphate v_1, and carbonate v_1/Amide I [24].

Statistical Analysis

The measurements obtained from the integrated intensities, areas under the Raman peaks and ratios of these bands, were analyzed using SPSS software version 11.0® (SPSS Inc, Chicago, Illinois, United States). The results are presented as means and standard deviations. The one-way ANOVA and the Tukey–Kramer multiple comparisons test were applied to check the significance of the mean value of Raman spectroscopic parameters between the bone sites of the OVX and SHAM groups. Differences were considered significant if $p<0.05$.

RESULTS

Raman Peak Parameters

The Raman spectrum shows prominent vibrational band related to tissue composition [24]. Fig. (**1**) shows an example of a spectrum of lumbar vertebral body in which the differences were most extreme. This typical Raman spectrum of bone from the SHAM and OVX groups showed that both had the same peak positions, but their intensity at certain Raman shifts were different. Also, the main Raman bands of bone tissue at 431, 589, 959, 1006, 1071, 1268, 1453, and 1668 cm^{-1} were consistent with previous results [22,28,29]. In the typical spectrum from bone, the band centered at 959 cm^{-1} corresponds to the symmetric stretching vibration (v_1) of phosphate (PO_4^{3-}) and is the strongest marker of bone mineral. The spectra displayed other Raman PO_4^{3-} vibration bands such as the v_2 symmetrical bending centered at 431 cm^{-1}, v_4 symmetrical bending centered at 589 cm^{-1}, and v_3 asymmetrical stretching mode centered at 1044 cm^{-1}. The band found at 1006 cm^{-1} was assigned to the v_1 mode of the organic phosphate associated with a phosphoprotein that occurs in low mineralization regions [30]. The peak at 1071 cm^{-1} was formed by the v_1 carbonate (CO_3^{2-}) vibrational mode and indicated the extent of carbonate incorporated into the hydroxiapatite lattice (type B carbonate substitution). The Raman peaks of collagen matrix are the Amide III (1268 cm^{-1}) and Amide I (1665 cm^{-1}), which arise largely from the collagen, and the CH_2 wag peak (1453 cm^{-1}) that is present in both collagenous and non-collagenous organic molecules.

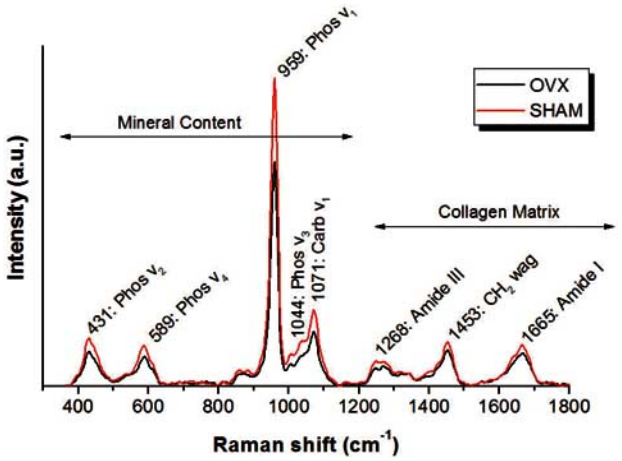

Fig. (1). Typical FT-Raman spectra from lumbar vertebral body of ovariectomized (OVX: gray line) and control (SHAM: black line) animals showing the major peaks and their molecular constituents.

Mineral and Matrix Content

The site-dependent variations of bone were noted in the ovariectomized and sham-operated spectra (Fig. **2**).

Fig. (**3A**) shows the results related to mineral content (PO_4^{3-} v_1: 959 cm^{-1}) for the SHAM and OVX groups. For the

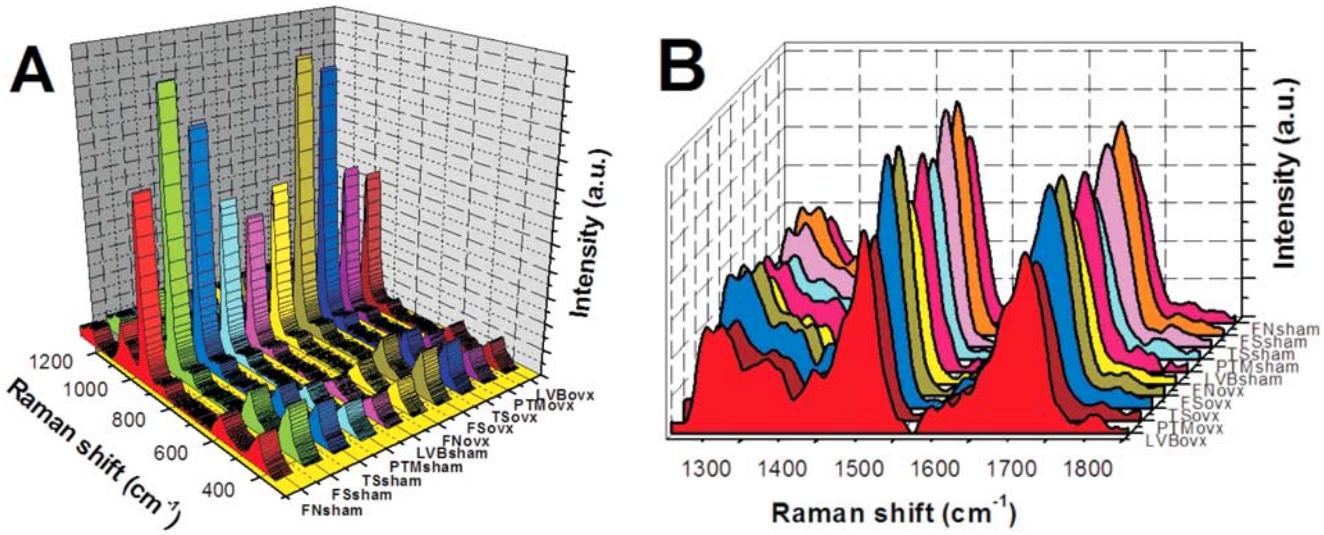

Fig. (2). Mean Raman shift of the sham-operated (SHAM) and ovariectomized (OVX) groups on different site bones. FN = femoral neck, FS= femoral mid-shaft, PTM = proximal tibial metaphysis, LVB = lumbar vertebral body. (**A**) Note the reduction of intensity of the main Raman peak centered at: 959 cm^{-1} (PO_4^{3-} υ1: marker of bone mineral content) after ovariectomy. (**B**) Spectral features of bone organic Raman bands.

FN, PTM, and LVB from the SHAM animals the intensity of the PO_4^{3-} v_1 peak was higher ($p<0.05$) than that from the OVX animals, however, this difference was not statically significant for the FS and TS bone sites. The FS and TS were found to be significantly greater for the FN, PTM, and LVB site bones in both groups. In addition to the main Raman marker of bone mineral (PO_4^{3-} v_1: 959 cm^{-1}), the others Raman peaks relationed to mineral content are represented in Table **1**. Although a reduction in mineral content mainly in FN, PTM, and LVB from the OVX group could be observed when compared to same bone sites from the SHAM group, these differences were not statically significant ($p>0.05$). However, just like with the PO_4^{3-} v_1 peak, FS and TS had higher intensity than the trabecular sites in both experimental groups ($p>0.05$).

Raman data analysis of the organic bone components revealed that, except for the intensity of the Raman peaks at 1453 cm^{-1} (CH_2 wag), the other two markers of collagen

Table 1. Bone Mineral and Organic Raman Bands Obtained from Sham-Operated (SHAM) and Ovariectomized (OVX) Groups (n=6 per Group)

Raman parameters	SHAM					OVX				
	FN	FS	PTM	TS	LVB	FN	FS	PTM	TS	LVB
PO_4^{3-} υ_2 (431 cm^{-1})	2.31 (0.39)	3.48 (0.51)	1.99 (0.45)	3.22 (0.48)	1.78 (0.34)	2.00 (0.21)	3.41 (0.25)	1.94 (0.25)	2.77 (0.71)	1.47 (0.14)
PO_4^{3-} υ_4 (589 cm^{-1})	1.84 (0.30)	2.81 (0.40)	1.66 (0.30)	2.57 (0.33)	1.55 (0.33)	1.65 (0.24)	2.80 (0.26)	1.53 (0.15)	2.28 (0.51)	1.23 (0.14)
PO_4^{3-} υ_1 (959 cm^{-1})	14.1 (2.47)	**21.25# (3.28)**	11.91 (2.69)	**20.00# (2.84)**	10.20 (2.34)	**9.35* (1.74)**	**21.14# (1.60)**	**5.65* (1.70)**	**17.78# (4.24)**	**5.64* (1.38)**
Phosphoprotein (1005 cm^{-1})	1.34 (0.18)	2.17 (0.33)	1.37 (0.17)	1.90 (0.20)	1.11 (0.16)	1.51 (0.14)	2.17 (0.22)	1.41 (0.19)	2.00 (0.41)	1.10 (0.16)
Carbonate (1071 cm^{-1})	4.38 (0.38)	**5.35# (0.79)**	3.13 (0.63)	**4.94# (0.63)**	3.57 (0.57)	**2.84* (0.37)**	**5.24# (0.43)**	3.04 (0.42)	**4.43# (0.89)**	**2.39* (0.38)**
PO_4^{3-} υ_3 (1044 cm^{-1})	2.16 (0.30)	3.22 (0.53)	1.91 (0.40)	3.10 (0.45)	1.74 (0.37)	1.92 (0.20)	3.17 (0.27)	1.89 (0.36)	2.77 (0.56)	1.51 (0.18)
Amide III (1268 cm^{-1})	1.42 (0.16)	1.73 (0.25)	1.36 (0.08)	1.67 (0.15)	1.30 (0.18)	1.43 (0.10)	2.02* (0.29)	1.39 (0.29)	2.07* (0.27)	1.32 (0.15)
CH_2 wag (1453 cm^{-1})	2.41 (0.29)	3.07 (0.41)	2.43 (0.12)	3.13 (0.29)	2.42 (0.36)	2.45 (0.21)	3.30 (0.61)	2.64 (0.46)	3.34 (0.46)	2.50 (0.39)
Amide I (1665 cm^{-1})	2.21 (0.25)	2.82 (0.36)	2.10 (0.14)	2.68 (0.22)	2.17 (0.28)	2.22 (0.16)	**3.39*** (0.36)	2.15 (0.38)	**3.22*** (0.32)	2.30 (0.27)

Note: the results are expressed as mean and standard deviations (SD) of integrated intensities (arbitrary units $\cdot 10^{-3}$). FN = femoral neck, FS= femoral mid-shaft, PTM = proximal tibial metaphysis, LVB = lumbar vertebral body.

Bold values indicates statistical significance:

*OVX group significantly lower than same bone site from SHAM group ($p<0.05$).

FS and TS bone sites significantly greater than FN, PTM and LVB bone sites ($p<0.05$).

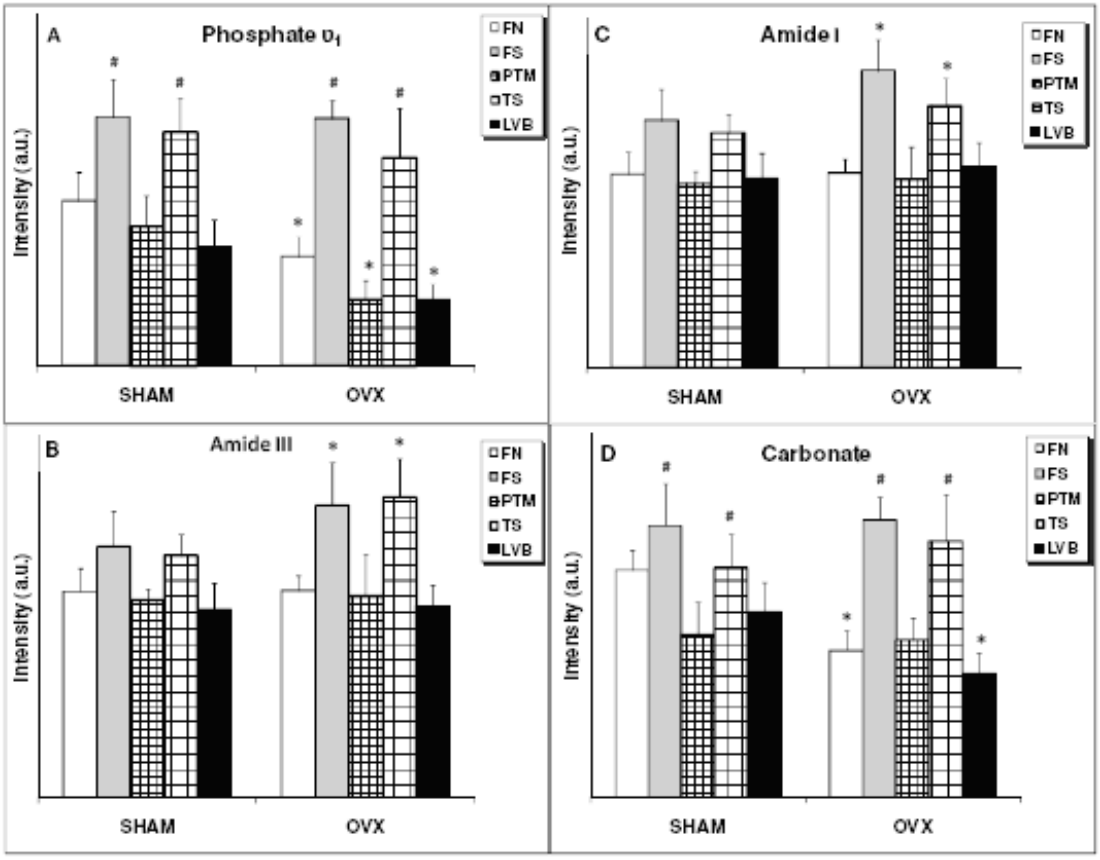

Fig. (3). Integrated intensity of Raman peaks on the bone sites from sham-operated (SHAM) and ovariectomized (OVX) groups (n=6 per group). The results are expressed as mean and standard deviations. a.u. = arbitrary units; FN = femoral neck, FS= femoral mid-shaft, PTM = proximal tibial metaphysis, LVB = lumbar vertebral body. (**A**) phosphate υ1 (959 cm^{-1}) and (D) Carbonate (1071 cm^{-1}) *OVX group significantly lower than same bone sites from SHAM group ($p<0.05$); # FS and TS bone sites significantly greater than FN, PTM and LVB bone sites ($p<0.05$). (**B**) Amide III (1268 cm^{-1}) and (**C**) Amide I (1665 cm^{-1}). **D**. * FS and TS bone sites significantly greater than other bone sites from SHAM and OVX group ($p<0.05$).

matrix (amide I and amide III) showed a significant increase ($p<0.05$) in FS and TS from the OVX group when compared to all other bone sites from the SHAM group (Figs. **3B** and **C**). FN, PTM, and LVB had a slight increase with the ovariectomy ($p>0.05$) (Table **1**).

Table **1** also indicates that the intensity of Raman peak centered at 1003-1005 cm^{-1} (phosphoprotein that occur in regions of low mineralization) does not differed significantly ($p>0.05$) between the SHAM and OVX groups. However, there were higher intensities in the OVX group and interestingly the FS and TS site showed the higher values regardless of experimental group.

Mineral to Matrix and Carbonation Ratios

The mineral to matrix ratio (phosphate v_1/Amide I) was only significantly lower in LVB from the OVX group when compared to same bone site from the SHAM group ($p<0.05$). Althought not significant, this same trend was observed between all regions studied: lower mineral to matrix ratio in femoral and tibial sites from the OVX group (Table **2**).

With regard to the Raman peak centered at 1071 cm^{-1} relationed to v_1 carbonate vibrational mode, the content (integrated intensity) of this bone component in the OVX group was significantly lower than that found in the SHAM group when the FN and LVB bone sites ($p<0.05$) were analyzed (Fig. **3D**). Fig. (**3D**) also demonstrates that the FS and TS slight increased in the OVX group when compared to the same bone sites in the SHAM group, and significantly greater than the other bone sites in both experimental groups. Moreover, when the band areas of carbonate/phosphate and carbonate/Amide I ratios were performed, the results indicated higher carbonate/phosphate ratio in the OVX group when compared with the SHAM animals, especially in the LVB bone site ($p<0.05$) (Table **2**). Table **2** also illustrates the greater carbonate/Amide I ratio in FS and TS compared with the FN, PTM, and LVB bone sites in same experimental group ($p<0.05$) and a slight decrease of this ratio ($p>0.05$) after ovariectomy when compared with the same bone site from the SHAM and OVX groups.

DISCUSSION AND CONCLUSION

A great need exists to further characterize the available animal models for PMO to better understand the patho-genesis of the disease, investigate the new therapies, and diagnose osteoporotic bone. There has been extensive research on OVX rats including the histomorphometric changes, biochemical markers, bone densitometry, and evaluation of bone fragility [10-19]. However, little attention

Table 2. Comparison of Ratios of Raman Bands Areas from Bone Sites from Sham-Operated (SHAM) and Ovariectomized (OVX) Groups (n=6 per Group)

Raman ratios	SHAM					OVX				
	FN	FS	PTM	TS	LVB	FN	FS	PTM	TS	LVB
Mineral/Matrix	2.561 (0.447)	2.911 (0.209)	2.235 (0.453)	2.641 (0.16)	2.169 (0.302)	2.188 (0.147)	2.873 (0.153)	2.234 (0.170)	2.621 (0.159)	**1.500* (0.151)**
Carbonate/Phosphate	0.303 (0.052)	0.343 (0.073)	0.341 (0.012)	0.362 (0.011)	**0.425# (0.017)**	0.311 (0.058)	0.346 (0.072)	0.368 (0.013)	0.342 (0.015)	**0.467*# (0.014)**
Carbonate/Amide I	0.763 (0.157)	**1.001‡ (0.081)**	0.819 (0.158)	**0.911‡ (0.045)**	0.689 (0.193)	0.759 (0.057)	**1.000‡ (0.048)**	0.814 (0.064)	**0.902‡ (0.043)**	0.688 (0.169)

Note: the results are expressed as mean and standard deviations (SD) of bands areas from bone sites. FN = femoral neck, FS= femoral mid-shaft, PTM = proximal tibial metaphysis, LVB = lumbar vertebral body.
Bold values indicates statistical significance:
*OVX group significantly lower than SHAM group ($p<0.05$).
LVB bone site significantly greater than FN, FS, PTM and TS bone sites in same experimental group ($p<0.05$).
‡ FS and TS sites significantly greater than FN, PTM and LVB bone sites ($p<0.05$).

has been given to bone chemical composition changes especially taking into account the fact that not all bone sites (cortical and trabecular) of the rat skeleton lose bone at same rate [7]. Accordingly, the purpose of this study was to investigate the effects of ovariectomized rat model of PMO (the most commonly used animal model for osteoporosis) on bone chemical composition using FT-Raman spectroscopy on the surface of different bone sites.

Following ovariectomy, rapid loss of bone mass occurred similar to the bone changes that occur in the skeleton of women with postmenopausal osteoporosis [5,6]. The primary indication of osteoporosis is bone loss, which can be measured by decreased BMD. Studies that measured this variable in rats detected a significant reduction of mineral content by 3 months after ovariectomy especially in trabecular bone sites [8,10-12]. However, not all bone sites in the rat exhibited such bone loss nor did all bone sites lose bone at the same rate [7]. For instance, the earliest significant trabecular bone loss in the FN, PTM, and LVB occurring at 30, 14, and 60 days, respectively [31]. In contrast, ovariectomy-induced bone loss did not occur in cortical bone site [32]. It is interesting to note that the FN, PTM, and LVB are mainly compose of trabecular bone while FS and TS site bones are compose of cortical bone; these characteristics are fundamental to the results found in this study.

Vibrational spectroscopy has been used to analyze and classify the molecular constitution of mineral and matrix phases in bones and other mineralized tissues [22,33]. Currently, the Fourier transform infrared (FT-IR) and FT-Raman are the main vibrational spectroscopy techniques which have been successfully applied to study normal and osteoporotic tissue [20-30,34,35]. In comparison with FTIR, Raman spectroscopy has proven particularly useful because of its ability to be used on intact specimens as well as for its higher resolution and lesser interference from water. FT-Raman spectroscopic study of bone also simultaneously provides information about mineral and matrix components, which are not supplied by conventional methods [24,27]. Since the intensities of peaks are proportional to the relative amounts of the related species in vibrational spectroscopy [26], all major intensities of Raman peaks listed in Fig. (**1**) were selected to compare the degree of relative mineral and matrix content between the normal and osteoporotic bone (Table **1**). So, the higher intensity represents a higher concentration of mineral or matrix content.

The results of this study demonstrated that 3 months after ovariectomy there were differences in the chemical composition of all bone sites analyzed, especially when the phosphate v_1 (959 cm^{-1}), carbonate (1071 cm^{-1}), amide III (1268 cm^{-1}), and amide I (1665 cm^{-1}) Raman peaks (Fig. **3**) were considered. FT-Raman spectroscopy showed a decreased level of phosphate v_1 and carbonate content present in FN, PTM, and LVB (trabecular bone sites) from the OVX animals compared to the SHAM animals. In addition, for the FS and TS (cortical bone sites), the phosphate v_1 and carbonate content were greater when compared with the other site bones independent of experimental group.

Considering the reduction of mineral content of trabecular bone in the OXV rats observed by BMD [8,10-12], the intensity reduction of the main Raman marker peak of bone mineral content (PO_4^{3-} v_1: 959 cm^{-1}) after ovariectomy only in trabecular bone sites (FN, PTM and LVB) observed in this study (Fig. **3A**), indicates the monitoring ability of bone changes by FT-Raman and suggests the effectiveness of the surgery. Using others animal models to induce osteoporosis, Shen *et al.* [27] and Apeldoorn *et al.* [36] also demonstrated a severe intensity decreased of this bone mineral Raman band (~960 cm^{-1}) when compared to the control group. The other Raman PO_4^{3-} vibration (431 cm^{-1}, 589 and 1044 cm^{-1}) bone mineral markers from the OVX group listed in table 1, also had a reduction in mineral content in the trabecular bone sites although insignificant ($p>0.05$). It is probable that these Raman PO_4^{3-} vibrations were associated with labile and nonapatitic phosphate species in immature bone and indicate the possible existence of bone precursors that the ovariectomy appearance does not directly affect [22]. Thus, the estimation of phosphate v_1 vibration by FT-Raman is much more precise than that obtained by other mode of phosphate vibration.

There was a high level of remodeling in the trabecular bone region after ovariectomy [8,10-12] and not surprisingly the carbonate content was also affected in the FN, PTM, and LVB bone sites (Fig. **3D**). A decrease in the total carbonate content in osteoporotic bone has already been reported [37]. The Raman band centered at 1070 cm^{-1} indicates the amount of type B carbonate substitution in the mineral crystals, which is associated with aging [28]. It is probable that the ovariectomized animals may have accentuated the selective resorption of older, more mature bone mineral, which contains a higher concentration of carbonate than young bone [29]. In fact, the osteoporosis process seems to involve an advanced bone that would be considered immature but older [22].

In contrast with the present study, Bohic and Rey [29] have compared rats treated with bisphosphonate to untreated ovariectomized rats, found no change in the mineral or carbonate content using different techniques including FT-Raman spectroscopy. However, they used a bone defatted powder and for this reason, we believed that the real nature of the bone tissue could be compromised not allowing direct comparisons with this study.

The variation in bone organic matrix observed in the figure 3B and C indicates that collagen type I content was changed after ovariectomy in only the cortical bone sites (FS and TS). The bone growth ovariectomy-stimulated on periosteal probably affected the results [38]. It is important to distinguish the remodeling of the adult skeleton from the growth at the periosteal surface. In the last case, new bone formation, which is a sequencial process involving proliferation, formation, and then mineralization of the extracellular matrix, occurs without prior osteoclastic action [39]. On the other hand, the mid-diaphyseal endosteum in the OVX rats exhibited increased bone resorption by osteoclastic action. As a result of these combined changes, cortical bone slowly changes and techniques such as DXA fail to demonstrate the osteoporosis [7]. Many non-collagenous proteins synthesized by the osteoblasts are also incorporated into the bone matrix and the CH_2 wag Raman peak (1453 cm^{-1}) could illustrate any variation [23]. However, a significant increase in this marker was not observed until 3 months post ovariectomy (Table **1**) which indicates that the measurement of amide III (1268 cm^{-1}) and amide I (1665 cm^{-1}) Raman peaks by FT-Raman spectroscopy should be encouraged to observe the cortical ovariectomy-induced alterations. Also, the Raman peak centered at 1003-1005cm^{-1} which is related to a phosphoprotein that occurs in regions of low mineralization does not adequately indicate the effects of the ovariectomy (Table **1**).

Considering the Raman ratios, a lower mineral/matrix ratio and a higher carbonate/phosphate were observed in the OVX group. With the exception of LVB from the OVX group ($p<0.05$), the mineral to matrix ratio (phosphate v_1/Amide I) was not significantly different between the experimental groups. However, the same trend was observed in all regions studied: lower mineral to matrix ratio in femoral and tibial sites from the OVX group. The similarity of the results for all site bones must be contrasted the following way. In the case of the trabecular sites (FN, PTM, and LVB), the ovariectomy caused reduction in mineral content and the reduction of mineral to matrix ratio was directly proportional. In the case of the cortical sites (FS and TS), the ovariectomy did not reduce mineral content but increased the Raman peak of Amide I, so this reduction of mineral to matrix ratio was inversely related. Thus, the trend towards decreased mineral/matrix ratio seems to suggest the possibility that the ovariectomy caused specific chemical changes in the bone sites, which indicates some degree of remodeling specially in the trabecular bone sites.

Bone mineral is metabolically active, thus numerous interactions between ions from the extracellular fluid and ions that constitute the apatite crystals are possible. The carbonate/phosphate ratio appears to be a key variable in osteoporotic fracture [40]. McCreadie *et al.* observed a greater carbonate/phosphate ratio in iliac crest cortical bone from women with fractures [25]. Using FT-IR, Boskey *et al.* compared iliac crest biopsies from women with post-menopausal osteoporosis, with iliac crest tissue from individuals without evidence of metabolic bone disease, and demonstrated significant differences in mineral crystal size/perfection (increased in osteoporosis) [41]. Using Fourier transform infrared microspectroscopy (FT-IRM), Gadeleta *et al.* demonstrated that the mineral crystals in both OVX monkeys and osteoporotic humans were larger, more crystalline, and had a greater carbonate/phosphate ratio than control and nonosteoporotic humans [35]. Paschalis *et al.* also reported similar results for human osteonal bone [34]. Thus, the results of the present study represent differences that may be attributed to the quality of bone tissue and may prove to be additional information about bone fragility and fracture risk.

Little attention have been given to the carbonate/Amide I ratio. Our results demonstrated that the cortical bone sites (FS and TS) showed greater values when compared with the trabecular bone sites in the same experimental group (Table **2**). This difference is consistent with cortical appearing "older" than trabecular bone because of the slower turnover rate [26].

Because of the extensive variation between the various site-bone and bone types, experimental methods that yield highly comprehensive information with minimal difficulty are desirable. Vibrational spectroscopy is an extremely useful tool in this endeavor. So, the direct bone compositional information obtained by FT-Raman would help to understand how the ovariectomized rat model of PMO affects the local chemical variations, thus further clarifying the mechanism of OVX-induced osteoporosis in rats. However, additional work utilizing other traditional techniques of bone analysis, therapeutic interventions, and medication are required to further clarify the chemical composition of the bone tissue after ovariectomy. In conclusion, the present study demonstrated that FT-Raman spectroscopy can be used to evaluate the bone alterations induced by this experimental model.

REFERENCES

[1] Raisz LG. Pathogenesis of osteoporosis: concepts, conflicts, and prospects. J Clin Invest 2005; 115: 3318-25.

[2] Johnell O, Kanis J. Epidemiology of osteoporotic fractures. Osteoporos Int 2005; 16: 3-7.

[3] World Health Organization. Assessment of fracture risk and its application to screening for postmenopausal osteoporosis. Technical Report Series. WHO, Geneva 1994.
[4] Carneiro RA. Epidemiological aspects of osteoporosis in Brazil. Bone 2001; 29: 298.
[5] Turner AS. Animal models of osteoporosis - necessity and limitations. Eur Cell Mater 2001; 22:66-81.
[6] Turner RT, Maran A, Lotinun S, *et al.* Animal models for osteoporosis. Rev Endocr Metab Disord 2001; 2: 117-27.
[7] Jee WSS, Yao W. Overview: animal models of osteopenia and osteoporosis. J Musculoskel Neuron Interact 2001; 1: 193-207.
[8] Kalu DN. The ovariectomized rat as a model of postmenopausal osteopenia. Bone Miner 1991; 15: 175-91.
[9] Recker RR, Barger-Lux, MJ. The elusive concept of bone quality. Curr Osteoporos Rep 2004; 2: 97-100.
[10] Braun MJ, Reiners C, Schiel H, Allolio B. Changes in biomechanical properties of rat femora induced by ovariectomy as analyzed by pQCT. Osteoporos Int 1996; 6:194.
[11] Sheng ZF, Dai RC, Wu XP, Fang LN, Fan HJ, Liao EY. Regionally specific compensation for bone loss in the tibial trabeculae of estrogen-deficient rats. Acta Radiol 2007; 48: 531-9.
[12] Pajamäki I, Sievänen H, Kannus P, Jokihaara J, Vuohelainen T, Järvinen TL. Skeletal effects of estrogen and mechanical loading are structurally distinct. Bone 2008; 43: 748-57.
[13] Lesclous P, Guez D, Baroukh B, Vignery A, Saffar JL. Histamine participates in the early phase of trabecular bone loss in ovariectomized rats. Bone 2004; 34: 91-9.
[14] Takayama B, Kikuchi S, Konno S, Sekiguchi M. An immunohistochemical study of the antinociceptive effect of calcitonin in ovariectomized rats. BMC Musculoskelet Disord 2008; 15:164.
[15] Reginster JY, Collette J, Neuprez A, Zegels B, Deroisy R, Bruyere O. Role of biochemical markers of bone turnover as prognostic indicator of successful osteoporosis therapy. Bone 2008; 42: 832-6.
[16] Eastell R, Hannon RA. Biomarkers of bone health and osteoporosis risk. Proc Nutr Soc 2008; 67: 157-62.
[17] Fuchs RK, Allen MR, Condon KW, *et al.* Strontium ranelate does not stimulate bone formation in ovariectomized rats. Osteoporos Int 2008; 19: 1815-7.
[18] Bauss F, Lalla S, Endele R, Hothorn LA. Effects of treatment with ibandronate on bone mass, architecture, biomechanical properties, and bone concentration of ibandronate in ovariectomized aged rats. J Rheumatol 2002; 29: 2200-8.
[19] Haque T, Uludag H, Zernicke RF, Winn SR, Sebald W. Bone marrow cells from normal and ovariectomized rats respond differently to basic fibroblast growth factor and bone morphogenetic protein 2 treatment in vitro. Tissue Eng 2005; 11: 634-44.
[20] Ammann P, Rizzoli R. Bone strength and its determinants. Osteoporos Int 2003; 14: 13-18.
[21] Boivin G, Meunier PJ. The mineralization of bone tissue: A forgotten dimension in osteoporosis research. Osteoporos Int 2003; 14: 19-24.
[22] Carden A, Morris MD. Application of vibrational spectroscopy to the study of mineralized tissues (review). J Biomed Optics 2000; 5:259-68.
[23] Faibish D, Ott SM, Boskey AL. Mineral changes in osteoporosis a Review. Clin Orthop Relat Res 2006; 443:28–38.
[24] Smith R, Rehman I. Fourier transform Raman spectroscopic studies of human bone. J Mater Sci Mater Med 1995; 5:775-8.
[25] Mccreadie BR, Morris MD, Chen TC, *et al.* Bone tissue compositional differences in women with and without osteoporotic fracture. Bone 2006; 39: 1190-5.
[26] Goodyear SR, Gibson IR, Skakle JMS, Wells RPK, Aspden RM. A comparison of cortical and trabecular bone from C57 black 6 mice using Raman spectroscopy. Bone 2009; 44: 899-907.
[27] Shen J, Fan L, Yang J, Shen AG, Hu JM. A longitudinal Raman microspectroscopic study of osteoporosis induced by spinal cord injury. Osteoporos Int, Published online May 13, 2009; Available as doi 10.1007/s00198-009-0949-3;
[28] Akkus O, Adar F, Schaffler MB. Age-related changes in physico-chemical properties of mineral crystals are related to impaired mechanical function of cortical bone. Bone 2004; 34: 443-53.
[29] Bohic S, Rey C. Legrand A, *et al.* Characterization of the trabecular rat bone mineral: effect of ovariectomy and bisphosphonate treatment. Bone 2000; 26: 341-8.
[30] Sauer GR, Zunic WB, Durig JR, Wuthier RE. Fourier transform raman spectroscopy of synthetic and biological calcium phosphates. Calcif Tissue Int 1994; 54: 414-20.
[31] Wronski TJ, Cintron M, Dann LM. Temporal relationship between bone loss and increased bone turnover in ovariectomized rats. Calcif Tissue Int 1988; 42:179-83.
[32] Miyakoshi N, Sato K, Tsuchida T, Tamura Y, Kudo T. Histomorphometric evaluation of the effects of ovariectomy on bone turnover in rat caudal vertebrae. Calcif Tissue Int 1999; 64: 318-24.
[33] Santanna GR, Santos EAP, Soares LES, *et al.* Dental enamel irradiated with infra-red diode laser and photo absorbing cream: part 1- FT-Raman study. Photomed Laser Surg 2009; 27:499-507.
[34] Paschalis EP, Betts F, Dicarlo E, Mendelsohn R, Boskey AL. FTIR microspectroscopic analysis of human iliac crest biopsies from untreated osteoporotic bone. Calcif Tissue Int 1997; 61: 487-92.
[35] Gadeleta SJ, Boskey AL, Paschalis E, Carlson C, Menschik F, Baldini TA. Physical, chemical, and mechanical study of lumbar vertebrae from normal, ovariectomized and nandrolone decanoate-treated cynomolgus monkeys (Macaca fasciculares). Bone 2000; 27: 541-50.
[36] Van Apeldoorn AA, De Boer J, Van Steeg H, Hoeijmakers JHJ, Otto C, Van Blitterswijk CA. Physicochemical composition of osteoporotic bone in the trichothiodystrophy premature aging mouse determined by confocal raman microscopy. J Gerontol A Biol Sci Med Sci 2007; 62: 34-40.
[37] Thompson DD, Posner AS, Laughlin WS, Blumenthal NC. Comparison of bone apatite in osteoporotic and normal Eskimos. Calcif Tissue Int 1983; 35: 392-3.
[38] Turner RT, Vandersteenhoven JJ, Bell NH. The effects of ovariectomy and 17 beta estradiol on cortical bone histomorphometry in growing rats. J Bone Miner Res 1987; 2: 115-22.
[39] Matsuo K, Irir E. Osteoclast-osteoblast communication. Arch Biochem Biophys 2008; 473: 201-9.
[40] Freeman JJ, Wopenka B, Silva MJ, Pasteris JD. Raman spectroscopic detection of changes in bioapatite in mouse femora as a function of age and in vitro fluoride treatment. Calcif Tissue Int 2001; 68: 156-62.
[41] Boskey AL, Dicarlo E, Paschalis E, West P, Mendelsohn R. Comparison of mineral quality and quantity in iliac crest biopsies from high- and low-turnover osteoporosis: an FT-IR microspectroscopic investigation. Osteoporos Int 2005; 16: 2031-8.

Received: September 30, 2009 Revised: January 25, 2010 Accepted: February 11, 2010